INTERNATIONAL JOURNAL OF PROGRESSIVE RESEARCH IN ENGINEERING MANAGEMENT AND SCIENCE (IJPREMS)

www.ijprems.com
editor@ijprems.com

Vol. 03, Issue 10, October 2023, pp : 335-344

e-ISSN : 2583-1062

Impact Factor : 5.725

DEVELOPMENT AND PERFORMANCE EVALUATION OF AN INSTRUMENTED SOIL HARDPAN BREAKER

Abisuwa T. A[1]

[1]Department of Agricultural and Bio-Environmental Engineering Rufus Giwa Polytechnic, Owo Ondo State, Nigeria.

Corresponding Email: abibayo2014@gmail.com

DOI: https://www.doi.org/10.58257/IJPREMS32162

ABSTRACT

Straight shank subsoiler (SSS) instrumented subsoilers was developed for alleviation of compaction on agricultural land. Draughts and soil disturbance of the subsoilers were measured during operation in as sandy clay loam soil. The SSS was designed and constructed for use by the tool carrier in loosening soil hard pan. Shanks from the machine were hitched to the tool bar of the carrier. A 100 kN calibrated load cell was connected to the tool carrier via the drawbar of a 36 kW, 4-wheel drive new Holland tractor and operated at three different speeds; 1.1, 1.6 and 2.5 Km/h. The load cell was connected to the data logger via instrumentation amplifier. Laptop computer system was connected to the data *logger* to download the draught data for each shank which was operated at four levels of depth; 9, 18, 27, 36 and 45 cm. Results showed that the penetration resistance reduced after the soil loosening. The trend of draught measurement during field operation showed that the draught force increases with soil depth for the operating speed at 1.1 and 1.6 Km/h, while there was reduction with soil depth at 2.5 Km/h. This result showed that the use of Straight shank subsoiler (SSS) is dependent on the operating speed of the tractor.

Keywords: subsoilers, soil depth, draughts, hard-pan

1. INTRODUCTION

Tillage is one of the basic and essential operations in agricultural production. The aim of tillage is to give the optimum environment for germination and crop development and to enable mechanization and soil and water management practices to take place. Hard pan or soil pan is a dense layer of soil usually found below the uppermost topsoil layer are wide spread problems that limit crop production. Normally, compaction is the result of heavy machinery compressing the soils. Heavily compacted soils contain few large pores and have a reduced rate of both water infiltration and drainage from the compacted layer. The change in pore space restricts root growth, and the gas exchange necessary for plant growth and yield. Compaction restricts infiltration of water, increasing runoff and erosion, leading to the loss of valuable nutrients (Manuwa et al., 2011). According to Ademosun et al. (2014), soil compaction refers to the formation of well packed soil, often at the bottom of the cultivated layer. Causes of soil compaction include rain drop impact, natural processes, wheel traffic, tillage operation, pasture grazing and minimal or no crop rotation. It is seen as another form of land degradation a significant global issue during the 20th century and remains of high importance in the +21st century as it affects the environment, agronomic productivity, food security, and quality of life (Bandalan et al., 1999). Soil degradative processes include the loss of topsoil by the action of water or wind, chemical deterioration such as nutrient depletion, physical degradation such as compaction, and biological deterioration of natural resources including the reduction of soil biodiversity (Lal, 2001). Hard layers can be caused by traffic or soil genetic properties that result in horizons with high density or cemented soil particles (D‟Haene et al., 2008). This has the ability of resisting crop root penetration and reducing water and air flow. Consequently, leading to limited water and nutrient uptake, low water flow in the soil disables rainfall or irrigation water from entering into the soil profile where it can be available for plant use. In another part, insufficient aeration of the soil limit oxygen and carbon-dioxide exchange with the atmosphere there by limiting the access of plant and micro-organism respiration and consequently impeding crop production (Raper, 2007) According to UN Food and Agriculture Organization 2005, In West Africa, Nigeria in particular, human-induced soil degradation is a common phenomenon, its severity is light for 37.5% of the area (342,917 km2), moderate for 4.3% (39,440 km2), high for 26.3% (240,495 km2), and very high for 27.9% (255,167 km2) Soil erosion is the most widespread type of soil degradation in the country and has been recognized for a long time as a serious problem . In 1989, 693,000 km2 were already characterized by runoff-induced soil loss in the south and 231,000 km2 were degraded, mainly by wind erosion, in the north. Sheet erosion dominates all over the country, whereas rill and gully erosion are common in the eastern part and along rivers in northern Nigeria (Manor and Clark, 2001). Therefore, due to the degradation effect of soil erosion and compaction on the soil, which in some cases could lead to hard pan development, there is a need to develop a subsoiler for the loosening of the soil. The objective of this study is to evaluate the performance of a developed hardpan subsoiler at different soil depth and operating speed with respect to direction.

INTERNATIONAL JOURNAL OF PROGRESSIVE RESEARCH IN ENGINEERING MANAGEMENT AND SCIENCE (IJPREMS)

e-ISSN : 2583-1062

Impact Factor : 5.725

www.ijprems.com
editor@ijprems.com

Vol. 03, Issue 10, October 2023, pp : 335-344

2. MATERIALS AND METHOD

2.1 Description of the subsoiler and other components

The components of the machine encompass of the following; shank, share, frame unit, hitch unit, hitch pin, rotary cultivator, circular tick plate, blade, drive shaft, and the drive unit (Figure 1). The dimensions of the components of the machine is as illustrated below

The shank: 100 × 120 ×700 mm was machined in order to shape it to accommodate the shoe which made up of medium carbon steel 100×100×10mm

Share: - This was forged to be fixed into the shoe and it made up of high carbon steel with dimension of 100×20 mm

Frame unit: - The frame made up of hollow square milled steel pipe 100×100 mm 80×80 mm. The frame was cut into sizes and welded to form the shape required to accommodate other components.

Hitch unit: - This was made up of milled steel plate bar of 3000×100×10 mm and was cut to size and welded to the frame.

Hitch pin: - The hitch pin which was used for connecting components together was with a dimension of 30 × 200 mm.

Rotary cultivator: This consist of 8 (eight) circular tick plates of (200×10 mm) welded to a drive shaft (50 mm) and carried 40 cuter blades at its periphery.

Circular tick plate: This was made of 200×10 mm, and was machined and drilled to accommodate 16 holes for the blades and it is made up of milled steel.

Blade: This is made up of high carbon steel and forged to shape

Drive shaft: This was made up of carbon steel with 50 mm diameter, and was turned on the latte machine.

The drive unit: - It was made of a gear box, PTO drive shaft, chain sprocket and chain curve.

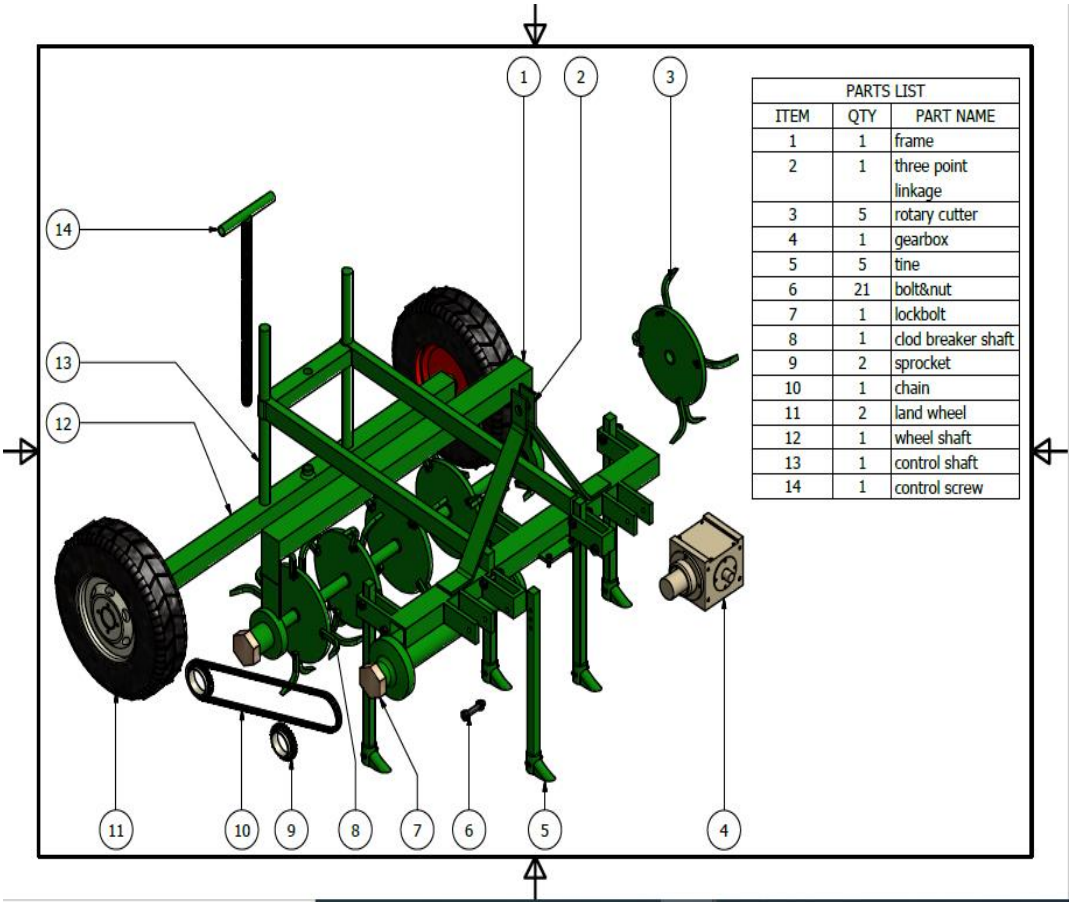

PARTS LIST		
ITEM	QTY	PART NAME
1	1	frame
2	1	three point linkage
3	5	rotary cutter
4	1	gearbox
5	5	tine
6	21	bolt&nut
7	1	lockbolt
8	1	clod breaker shaft
9	2	sprocket
10	1	chain
11	2	land wheel
12	1	wheel shaft
13	1	control shaft
14	1	control screw

Figure 1: Description of the machine components with the subsoiler

2.2 Design Analysis

2.2.1 Frame design

The volume of the frame was determined as 0.016m^3 using equation 1. The weight of the frame was determined as 125.4744kg using equation 2 and the weight of the frame was determined as 1237.18N using the appropriate equation as follows.

INTERNATIONAL JOURNAL OF PROGRESSIVE RESEARCH IN ENGINEERING MANAGEMENT AND SCIENCE (IJPREMS)

e-ISSN : 2583-1062

Impact Factor : 5.725

www.ijprems.com
editor@ijprems.com

Vol. 03, Issue 10, October 2023, pp : 335-344

Volume of the frame

Volume = surface area x thickness of the material = 0.015984m^3

Mass = ρgh (1)

Weight of the Frame

To determine the weight of the frame, it is important to determine the surface area and the volume of the frame materials.

Surface Area of the frame – SA_f (2)

Surface Area = Length x width

= 0.3996m^2

Volume of the frame material V_{fm}

$V_{fm} = SA_f \times t_m$ (3)

= 0.016m^3

Where t_m is 1.200m (thickness of the milled steel used)

Mass of the frame material M_{mf}

According to Aniel et al 2016 the mass and weight of the frame material can be determined by using equations (x and y)

$M_{fm} = V_{fm} \times \rho$ (4)

M_{fm} = 125.4744

Where ρ is 7850 (density of mild steel)

To determine the weight of the frame material

$W_{fm} = M_{fm} \times g$ (5)

= 1237.18N

Where g is the acceleration due to gravity.

The weight of the frame is therefore 1237.18N

2.2.2 Design of clod pulverizer frame

The volume of the frame was determined as 0.009 m^3 using equation 1, the mass of the frame was determined as 75.637 kg using equation 2 and the weight of the frame was determined as 742.00N using appropriate equation as follows:

Volume of the frame $_{clod\ pulverizer}$

Vol $_{clod\ pulverizer}$ = surface are x thickness of the material

= 0.009 m^3

Mass =ρgh (6)

= 75.637 kg

To determine the weight of the frame, it was important to determine the surface area and the volume of the frame materials.

Surface Area of the frame$_{clod\ pulverizer}$

Surface Area of the frame materials

Surface Area of the frame = SA $_{clod\ pulverizer}$

Surface Area = length x width = 1.204 m^2

Volume of the frame material = $V_{cp} = SA_{cp} \times t_{cp}$ (7)

= 0.009 m^3

2.2.3 Determination of the weight of the land wheels

Average mass of passenger tire ranges between 15 – 20kg. Therefore, the mass of 2 wheels equal to 4 kgs

The weight is therefore

Mass x g = 392.4 N

Volume of the wheel shaft = Vol.$_{steel}$ = 2(Vol. of ABCD) + 2(Vol. of DCFE) (8)

Vol.$_{steel}$ (DCFE) 2 = (L x B x thickness) 2 (9)

= 0.0006 m^3

Total Vol. = 0.002 m^3

INTERNATIONAL JOURNAL OF PROGRESSIVE RESEARCH IN ENGINEERING MANAGEMENT AND SCIENCE (IJPREMS)

www.ijprems.com
editor@ijprems.com

Vol. 03, Issue 10, October 2023, pp : 335-344

e-ISSN : 2583-1062

Impact Factor : 5.725

Mass = ρgh

= 7.693kg

Weight = Mass x g

= 75.47N

Mass of frame material $_{\text{clod pulverizer}}$

Mass = ρgh

= 756373248 kg

Weight of frame material $_{\text{clod pulverizer}}$

Weight $_{cp}$ = Mass $_{cp}$ x g

2.2.4 Determination of the shaft diameter

The diameters of both the driving and the driven shafts of the rotary clod pulverizer unit were determined using equation 10 (Hall *et al.,* 1982). The diameters of both the driving and the driven shafts were each determined as 53 mm 31.5mm respectively. Therefore, shafts diameter of 55mm and 32mm were selected for each of the shafts as presented in Table 1.

$$d^3 = \frac{16}{\pi s_s}\sqrt{(k_b M_b)^2 + (K_t M_t)^2} \quad (10)$$

Where d is the shaft diameter, S_s is the allowable stress, 55 x 10^{-6} N/m^2 for mild cast steel M_b is the maximum bending; K_b is the shock and fatigue factor for bending moment, 1.5; K_t is the shock and fatigue factor for tensional moment, 1 and M_t is the maximum tensional moment.

The length speed, power and the capacity of the chain.

Basic power transmission by sprockets and chain is from the driving shaft to the driven shaft.

The chain pitch was calculated using the formula

$$\text{Chain pitch} = \frac{\text{centre distance of sprocke}}{\text{distance between centre sprocket}} \quad (11)$$

= 11.65mm

But since 12.70mm is the closest value for the table, a chain drive having a pitch of 12.7mm has a projected bearing are of minimum breaking load of 390kg.

The diameter of the sprocket = 12.70mm

The chain velocity was calculated using chain velocity = pi × D× N / 60 (12)

3.4.3 Determination of the weight of the implement tine

No of tine is 5

Dimension of each Tine = 25 x 125 x 750

Thickness of each Tine = 25mm = 0.025m

Width = 125mm = 0.125m

Length = 78mm = 0.75m

Volume of each was calculated using

Vol_t = surface $area_t$ x thickness (13)

= 0.09375m^2

Volume of $material_t$

= surface area x thickness

= 0.023 m^3=

Mass = P_{steel} x Vol_{steel}

183.9 kg

Weight of each Tine = 1804.89 N

Weight of 5 Tines = 9024.43 N

= 9.02443 KN

2.3 Instrumentation System

The Instrumentation system for the automatic measurement of draught consists of a load cell that contains strain gauge elements and resistors (plate 1) and data acquisition components(plate 2) which include load cell amplifier that performs the function of amplification of electronic signal as sensed by the load cells; opto-coupler module for light emitting;

INTERNATIONAL JOURNAL OF PROGRESSIVE RESEARCH IN ENGINEERING MANAGEMENT AND SCIENCE (IJPREMS)

www.ijprems.com
editor@ijprems.com

Vol. 03, Issue 10, October 2023, pp : 335-344

e-ISSN : 2583-1062

Impact Factor : 5.725

micro-controller for precise motion control; LCD display for electronic digital display of values as measured by the system; SD-card shield for data storage and cable for wire connection between the system and the tractor. The system was designed to be powered by the battery of the tractor.

Plate 1: instrumentation panel

Plate 2: Instrumentation Digital display

Plate 3: installed 10-ton load cell on the Machine

2.3.1 Installation and circuitry works of instrumentation system

The load cell was installed on the frame of the hardpan breaker by bracket as presented in Plate 3 The components of the system were circuited at the Instrumentation Laboratory of the Department of Physics, Federal University of Technology, Akure. The system was calibrated in advance of being used for force measurement using a table vice loading method and the circuit diagrams for the load bridge strain gauge amplifier are presented in Figures 2

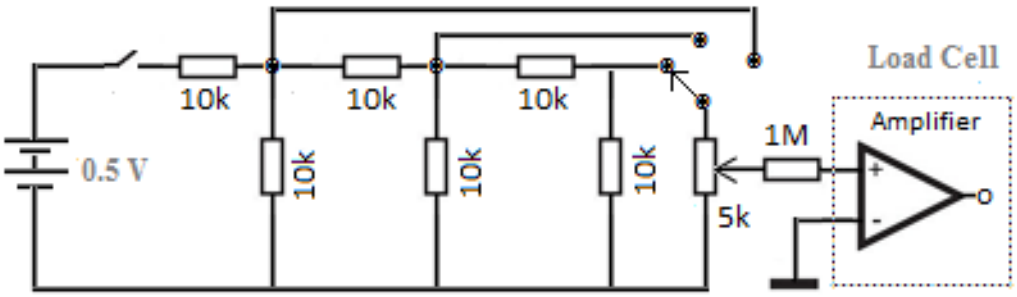

Figure 2: DC Voltage Attenuation with Load Amplifier

2.3.2 Testing and calibration of the milligram weighing system

Mounting the force measurement attachment on rigid tine on a compressed rectangular frame was used to test the reaction. The hydraulic jack was placed in between rigid tine and a typical 10 Ton load cell (Plate 4a and 4b). The strain gauge's output bridged circuit was linked to an amplifier. When the jack was gradually operated, the output voltage increased; when the jack was released, the output voltage decreased. Same procedure was repeated for the horizontal component (drag force) by rigid coupling on the tine carrying frame. The jack was placed horizontally alongside force exacted so when the jack was gradually operated, the output voltage increased; when the jack was released the output

INTERNATIONAL JOURNAL OF PROGRESSIVE RESEARCH IN ENGINEERING MANAGEMENT AND SCIENCE (IJPREMS)

e-ISSN : 2583-1062

Impact Factor : 5.725

www.ijprems.com
editor@ijprems.com

Vol. 03, Issue 10, October 2023, pp : 335-344

voltage decreased as presented in plate 4a. The arrangement shown on Plate 4b is the setting for vertical component (Z-axis) force calibration setting. As the jack is being operated gradually the corresponding output voltage from sensing output and force displaced by sensing standard load. Likewise, the arrangement shown on the Plate 2 is the setting for the calibration of horizontal axis (drag force). The corresponding output readings from the developed rigid tine force/voltage output and the standard load cell forces were analysed for both the vertical and the horizontal calibration systems.

Plate 3a : the horizontal calibration

Plate 3b : the vertical calibration

2.4 Description of the experimental site

The experiment was carried out on a sandy clay loam soil at the Federal University of Technology, Akure research farm, which is geographically located on the coordinate between the Latitudes of 7°17'0"N - 7°19'12"E and Longitudes of 5°7'0"E – 5°9'0"E.

3. RESULTS AND DISCUSSION

3.1 Bulk density and penetration resistance measurement before and after Subsoiling

The soil bulk density of the experimental site before and after experimentation is as illustrated in Table 1. Results showed that the soil bulk density increased down the soil depth. This might be as a result of the compactness of the soil at the deeper soil depths. After the use of the subsoiler, the soil became loosened, as evidenced by the lower bulk density value at each of the soil depth. This trend is agreement with the penetration resistance data, which is graphically presented in Figure 3. This corroborates the findings of Raper (2007) who reported reduced bulk density of soil after subsoiling. The penetration resistance increases as the soil depth increases, which is indicated by the positive slope indicated in the Figure below

Table 1: Soil bulk before and after the field experiment

Soil depth	Bulk density before penetration	Bulk density after penetration
9	1.32	1.21
18	1.25	1.17
27	1.33	1.25
36	1.37	1.27
45	1.52	1.28

The graphical illustration showed that the penetration reduced after the field experimentation, that is, loosening with the use of subsoiler. This result showed the effectiveness and the efficacy in the use of the subsoiler. Also, the result gave a coefficient of determination (R^2) of 0.937 and 0.941 for the relationship between the soil depth and penetration resistance before and after experimentation. These values of coefficient of determination showed that there is a good agreement between the soil depth and the penetration resistance.

INTERNATIONAL JOURNAL OF PROGRESSIVE RESEARCH IN ENGINEERING MANAGEMENT AND SCIENCE (IJPREMS)

www.ijprems.com
editor@ijprems.com

Vol. 03, Issue 10, October 2023, pp : 335-344

e-ISSN : 2583-1062

Impact Factor : 5.725

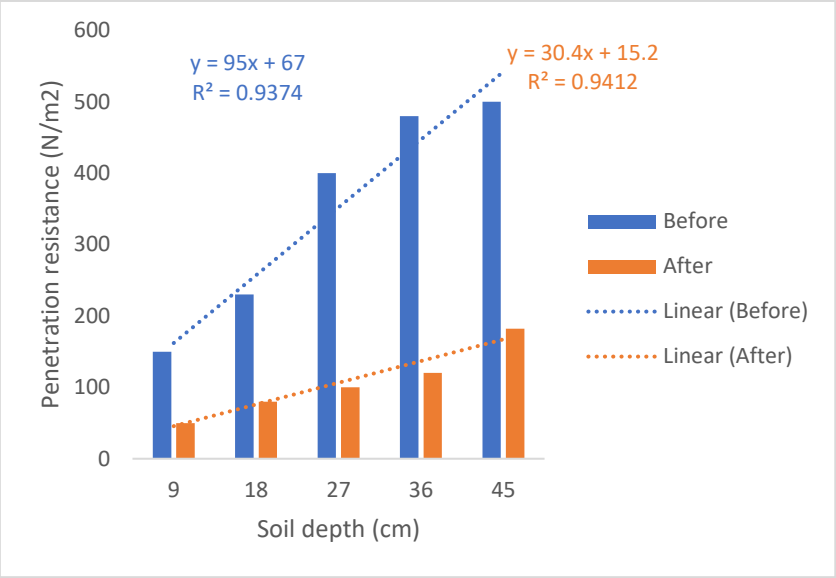

Figure 3: Penetration resistance before and after pulverization

3.2 Output Voltage of Load Cell Due to Load

Figures 4 and 5 show the graph of weight (N) and output voltage of instrumentation amplifier during calibration of the system. The relationship between the weight and the output voltage was expressed linearly. The coefficient of determinations (R^2) for the horizontal and vertical direction during calibration were 0.993 and 0.988, respectively. This high value of the R^2 showed that there was an excellent agreement and good for the prediction of the weight.

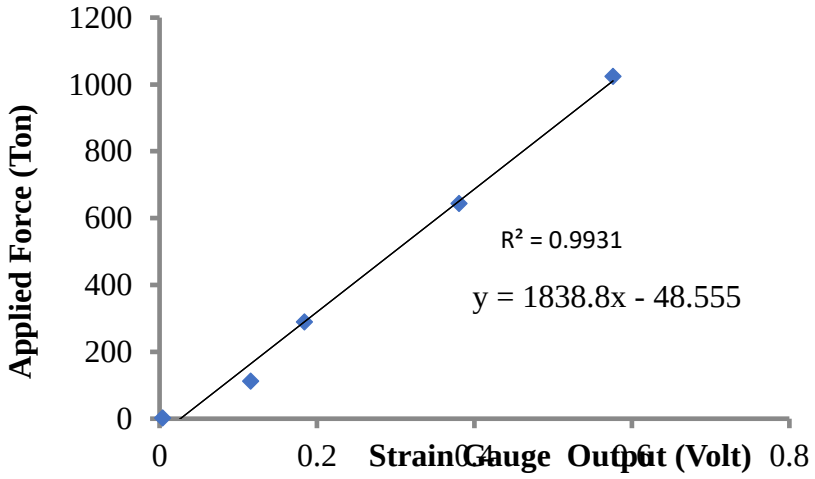

Figure 4 : Calibration Curve of Horizontal component (Drag Force) of Load Cell

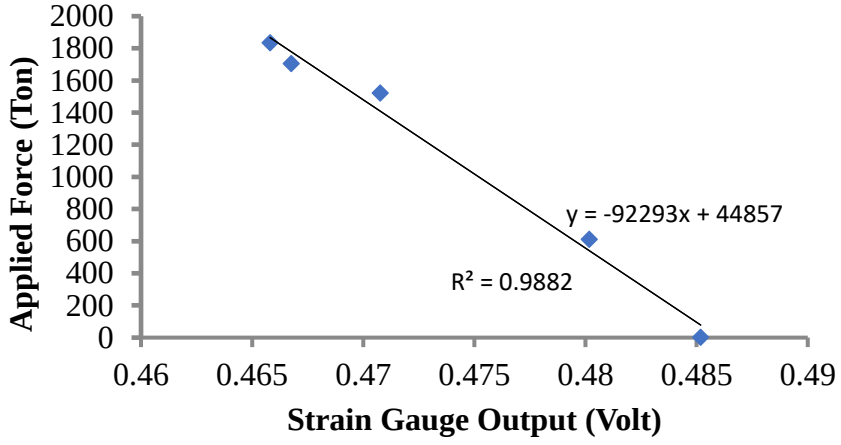

Figure 5 : Calibration Curve of the Vertical component (Z-Axis Force) of Load Cell

INTERNATIONAL JOURNAL OF PROGRESSIVE RESEARCH IN ENGINEERING MANAGEMENT AND SCIENCE (IJPREMS)

e-ISSN : 2583-1062

Impact Factor : 5.725

www.ijprems.com
editor@ijprems.com

Vol. 03, Issue 10, October 2023, pp : 335-344

3.3 Drag Force as a function of soil depth and speed at different direction of measurement

Table 2 below showed the average values of the drag force with respect to soil depth and with tractor speed at different speed of 1.1, 1.6 and 2.5 Km/h and at different direction. The result obtained from the instrument for the draft force showed that for the horizontal direction there was no significant difference ($P > 0.05$) for the implement driven with tractor at a speed of 1.1 Km/h. Similarly, there was no significant difference ($P > 0.05$) for horizontal speed on the draft force at 1.6 and 2.5 Km. However, Significant differences ($P < 0.05$) were observed in the effect of the speed on the draft forces in the vertical direction.

Table 2: Average values of draught (drag force; KN) at different depths with respect to direction (Horizontal and vertical) and speeds

	Speed (1.1 Km/h)		Speed (1.6 Km/h)		Speed (2.5 Km/h)	
	Horizontal	Vertical	Horizontal	Vertical	Horizontal	Vertical
Depth (cm)						
9	5.59a	9.48b	2.94a	9.17a	4.53a	56.0a
18	11.55a	8.76b	6.32a	10.69a	2.93a	9.14c
27	2.54a	33.09a	2.54a	33.09a	1.98a	13.54bc
34	5.83a	9.87b	2.94a	9.17a	3.74a	46.3ab
45	10.78a	16.77b	11.26a	50.50a	1.98a	13.54bc

*Mean that do not share the same letter are significantly different

For the horizontal speed at 1.1 Km/h, the highest value of the draft force was observed at 18 cm soil depth, while the lowest occurred at 27 cm soil depth, while the lowest and highest values were recorded at 18 cm and 27 cm for the vertical direction, respectively. For the speed of 1.6 Km/h, the lowest and lowest values were recorded at 27 cm and 45 cm in the horizontal direction, while it was observed at 9 and 45 cm in the vertical direction. Also, in the horizontal direction, the lowest and highest values of draft forces of 1.98 and 4.53 KN were recorded at 27 and 9 cm, respectively, while it was 13.54 and 56 KN at soil depth of 27 and 9 cm, respectively.

Therefore, due to inconsistency in the trend of increase/decrease in the draft force with respect to the soil depth and direction at the different speed, the graphical illustration of the relationship between the soil depth and draft force was plotted. The graphical illustrations for the different speeds (Figures 6 to 8) showed (confirmed) that there was truly inconsistency in the trend with the coefficient of determination (r^2) ranging between 0.058 and 0.47. However, the equation for the relationship between the soil depth and the draft showed a positive slope at draft speed of 1.1 and 1.6 Km/h, indicating that soil draft force increases with soil depth, therefore explaining the fact that the subsoiler was efficient and effective, even till soil depth of 45 cm. However, the speed of 2.5 Km/h showed a negative slope, indicating that some point down the soil depth, the efficiency and efficacy decreases at the speed of 2.5 Km/h. This is evident with highest value of draft force (56.0 and 4.53 KN in the vertical and horizontal direction) reported in Table 2 above.

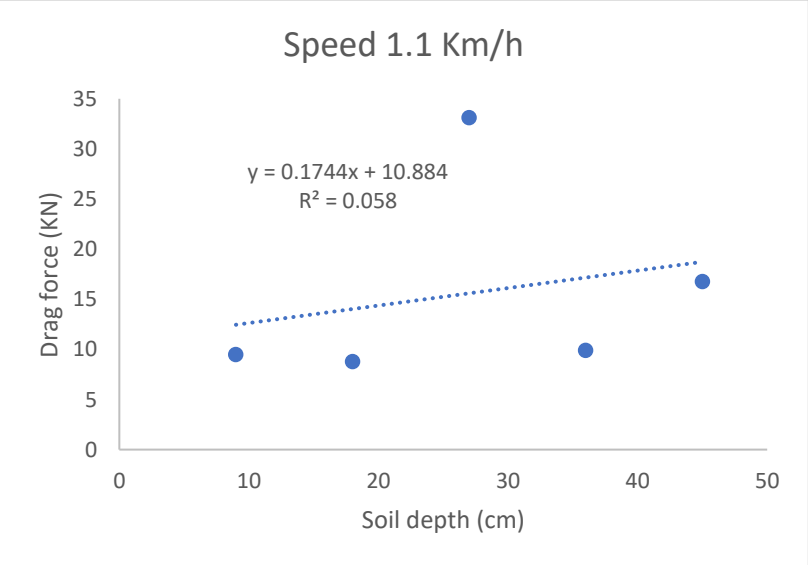

Figure .6 Trend of the drag force with respect to soil depth at a speed of 1.1 km/h for the vertical direction

INTERNATIONAL JOURNAL OF PROGRESSIVE RESEARCH IN ENGINEERING MANAGEMENT AND SCIENCE (IJPREMS)

www.ijprems.com
editor@ijprems.com

Vol. 03, Issue 10, October 2023, pp : 335-344

e-ISSN : 2583-1062

Impact Factor : 5.725

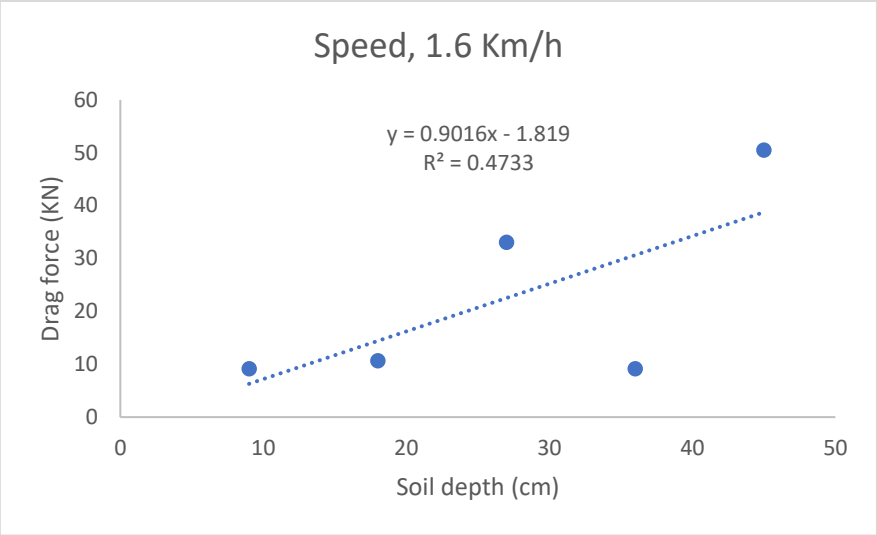

Figure.7. Trend of the drag force with respect to soil depth at a speed of 1.6 km/h for the vertical direction

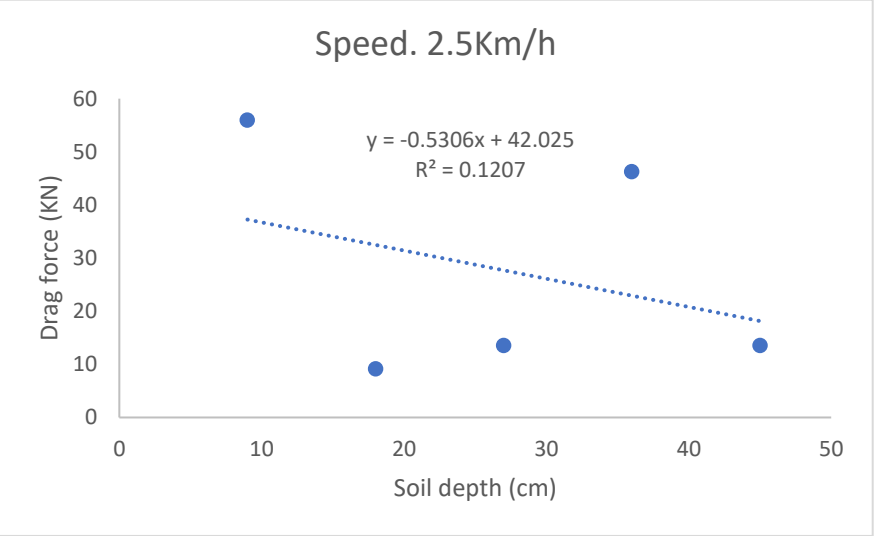

Figure.8: Trend of the drag force with respect to soil depth at a speed of 2.5 km/h for the vertical direction

The decreased trend observed for draft force at the 2.5 Km/h speed emphasized the handicapped or reduced efficacy nature of the SSS subsoiler at deeper depth of operation. This could be attributed to the surcharge or vertical pressure on the soil. This overburden pressure might have piled up, and then result in increased soil failure force. This observation is in agreements with the findings of some other researchers (Upadhyaya*et al.*, 1984; Kumar and Thakur, 2005). Similar result observed for the draft forces at both directions also occurred in the total draft force measured, including the trend of the equation, which indicate the relationship between the soil depth and the total draft force with the r^2 value ranging between 0.06 and 0.48 (Figure 9)

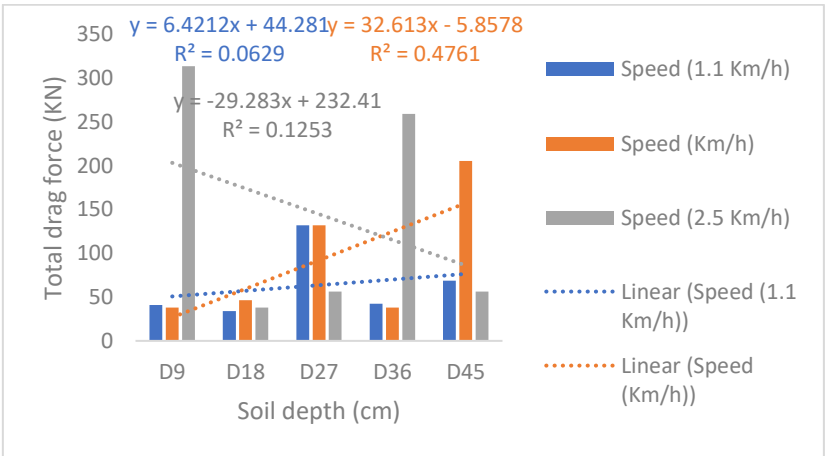

Figure 9: Graphical representation of the total drag force at different speeds

4. CONCLUSION

The following conclusion can be established from this study:

1. straight shank subsoiler was designed and their performance were evaluated.
2. Draught of subsoilers had high positive correlation with depth at speed of 1.1 and 1.6 Km/h and negative correlation with soil depth at 2.5 Km/h
3. The calibration equation established between weight and output voltage for the instrumentation was good.

5. REFERENCES

[1] Ademosun, O. C., Akande, L. O., Manuwa, S. I. and Ewetumo, T. (2014). Development of Liquid Animal Manure Injector Equipment with Instrumentation for Draught Measurement of Tillage Tools. Journal of Agricultural Engineering and Technology (JAET), Volume 22 (No.1).

[2] Bandalan, E. P., Salokhe, V. M., Gupta, C. P. and Niyamapa, T. (1999). Performance of an Oscillating Subsoiler in Breaking a Hardpan. Journal of Terramechanics: 36 (1999): 117-125.

[3] D"Haene, K., J. Vermang, W. M. Cornelis, B. L. M. Leroy, W. Schiettecatte, S. De Neve, D. Gabriels, G. Hofman (2008). Reduced tillage effects on physical properties of silt loam soils growing root crops. Soil & Tillage Res. 99, 279-290.

[4] Kumar, A. and Thakur, T. C. (2005). An investigation into comparative test of Conventional and winged Subsoilers. A Presentation at the ASAE Annual International Meeting, Tampa Convention Centre, Tampa, Florida, USA. ASAE Paper No. 051061.

[5] Manor, G. and Clark, R. L.(2001). Development of an Instrumented Subsoiler to Map Soil Hard-Pans and Real-Time Control of Subsoiler Depth. ASAE Annual International Meeting, Sacramento Convention Cente, Sacramento, California, USA, August, 2001.

[6] Manuwa, S.I., Ademosun, O.C., Agbetoye, L.A.S. and Adesina, A, 2011. Aspects of the development of outdoor soil bin facility (at FUTA) for soil Tillage Dynamics Research. Journal of Agricultural Engineering and Technology (JAET), 19(1): 1-8.

[7] Raper, R. L. (2007). In-row subsoilers that reduce soil compaction and residue disturbance. Publication of American Society of Agricultural and Biological Engineers (ASABE).Vol. 23(3): 253-258. ISSN 0883−8542.

[8] Upadhyaya, S. K., Williams, T. H., Kembie, L. J., Collins, N. E. (1984). Energy requirements for chiselling in coastal plain soils. Transaction of the American Society of Agricultural Engineers 27 (6), 1643-1649.